ARTICLE IN PRESS

Journal of Asian Earth Sciences xxx (xxxx) xxx–xxx

Contents lists available at ScienceDirect

Journal of Asian Earth Sciences

journal homepage: www.elsevier.com/locate/jseaes

Full length article

Mo-rich source and protracted crystallization of Late Mesozoic granites in the East Qinling porphyry Mo belt (central China): Constraints from zircon U/Pb ages and Hf-O isotopes

Zhiwei Bao[a,*], Mingfu Xiong[a,b], Qun Li[a,b]

[a] CAS Key Laboratory for Mineralogy and Metallogeny, Guangzhou Institute of Geochemistry, Chinese Academy of Sciences, Guangzhou 510640, China
[b] University of Chinese Academy of Sciences, Beijing 100049, China

ARTICLE INFO

Keywords:
East Qinling porphyry Mo belt
Late Mesozoic granites
Subducted continental crust of the Yangtze Block
Longevity of porphyry system
Mo-rich source

ABSTRACT

In the East Qinling orogenic belt, central China, there are numerous Mo deposits with over 6 *Mt* Mo metal. The giant Nannihu, Shangfanggou and Yuchiling porphyry Mo deposits are hosted in porphyry stocks associated with the Heyu batholith, whereas the giant Donggou porphyry Mo deposit is hosted in a stock associated with the Taishanmiao batholith. Zircon grains from the Heyu batholith have concordant $^{238}U/^{206}Pb$ ages scattered from 150 ± 3 to 130 ± 2 Ma with an age interval of nearly 20 m.y., whereas ore-hosting granitic porphyry stocks from the Nannihu, Shangfanggou and Yuchiling deposits have $^{206}Pb/^{238}U$ ages ranging from 151 ± 1 to 135 ± 1 Ma, 143 ± 1 to 132 ± 1 Ma, and 143 ± 5 to 131 ± 5 Ma, respectively. It is likely that the Heyu batholith has a prolonged history of incremental assembly and the ore-bearing granitic porphyry stocks may have originated from the same magma reservoir and emplaced in different stages. Likewise, zircon grains from the Taishanmiao batholith have concordant $^{238}U/^{206}Pb$ ages spanning in a period from 130 ± 2 to 111 ± 3 Ma, whereas those from the Donggou granitic porphyry stock have $^{238}U/^{206}Pb$ ages ranging from 125 ± 2 to 110 ± 3 Ma, nearly coeval with the Taishanmiao batholith. The molybdenite Re-Os model ages for each deposit are coincident with relatively young zircon $^{238}U/^{206}Pb$ ages of the host stock, indicating that Mo mineralization is likely related to late-stage magmatism. Zircon grains from the batholiths and granitic porphyry stocks have $\varepsilon_{Hf}(t)$ ranging from −10 to −30, $T_{DM}{}^2$ ages from 1.6 to 2.5 Ga and $\delta^{18}O$ from +5.0 to +8.7‰, which are taken to suggest the involvement of the subducted continental crust of the Yangtze Block in the source. We thus propose that the extensive Mo mineralization in the East Qinling porphyry Mo belt is genetically related to the prolonged granitic magmatism in the Late Mesozoic and a Mo-rich source that was related to the subducted continental crust of the Yangtze Block stagnating beneath the southern margin of the North China Craton.

1. Introduction

The East Qinling orogenic belt is the most important porphyry Mo ore belt in China, which hosts numerous Mo deposits with more than 6 M*t* Mo metal. Most of the Mo deposits are porphyry-type and genetically associated with Late Mesozoic granitic porphyries in the southern margin of the North China Craton, which were formed under an intracontinental orogenic regime. A genetic link of spatial- and temporal-associated porphyry Mo mineralization and Late Mesozoic granite magmatism in the East Qinling porphyry Mo belt has been investigated over the past decade (Bao et al., 2014, 2017; Gao et al., 2015; Li et al., 2007, 2017; Luo et al., 1991; Mao et al., 2008; Yang et al., 2013b; Ye et al., 2008a; Zhang et al., 2014b). The source of Mo and factors controlling the accumulation of large amounts of Mo are two major debated issues. Ore metals of porphyry Mo deposits are generally considered to have been originated from the same source as the host granite porphyry (e.g., Halter et al., 2005; Hedenquist and Lowenstern, 1994; Pettke et al., 2010), however, the source of Late Mesozoic granites that host porphyry Mo deposits in the East Qinling orogenic belt remains enigmatic. Many researchers considered that Late Mesozoic granites in the East Qinling orogenic belt were mainly derived from partial melting of the lower crust or Archean and Paleoproterozoic basement of the North China Craton, based on that the granitic rocks have whole-rock Nd model ages and zircon Hf model ages similar to the crystallization ages of the basement of the North China Craton (e.g., Li et al., 2012; Wang et al., 2013b, 2015, 2016a; Zhu et al., 2010, 2013). However, some researchers argued that many of these Nd and Hf model ages are substantially younger than the crystallization ages of the

* Corresponding author.
E-mail address: baozw@gig.ac.cn (Z. Bao).

https://doi.org/10.1016/j.jseaes.2017.12.022
Received 21 June 2017; Received in revised form 11 December 2017; Accepted 11 December 2017
1367-9120/

Please cite this article as: Bao, Z., Journal of Asian Earth Sciences (2017), https://doi.org/10.1016/j.jseaes.2017.12.022

basement and the mantle was isotopically enriched in the Late Mesozoic. They considered that Late Mesozoic granites were likely originated from the subducted continental crust of the Yangtze Block that was stacked beneath the southern margin of the North China Craton (e.g., Bao et al., 2009, 2014, 2017; Chen et al., 2013, 2015; Liu et al., 2015). Therefore, it is crucial to decipher the source of Late Mesozoic granites and to examine the factors that control Mo mineralization in the East Qinling orogenic belt.

Evidence from field observation, geochronology and geochemistry of many plutons indicates that they may have been constructed incrementally by amalgamation of pulses of magma over a period lasting for tens of thousands of years, or even millions of years (Coleman et al., 2016; Davis et al., 2012; Farina et al., 2012; Kaiser et al., 2017; Miller, 2008). For instance, the Tuolumne Intrusive Suite in California, U.S.A., was assembled over a period of at least 10 m.y. (Coleman et al., 2004). Porphyry ore mineralization related to granitic magmatism is commonly related to multiply replenishment of subvolcanic porphyry, vein opening and prolonged magmatic-hydrothermal processes (Rezeau et al., 2016; Sillitoe and Mortensen, 2010; von Quadt et al., 2011). There are four giant porphyry Mo deposits distributed closely in the East Qinling orogenic belt, including the Nannihu deposit with the ore reserve of 1.337 *Mt* at 0.096% Mo, Shangfanggou deposit of 0.726 M*t* at 0.134% Mo, Yuchiling deposit of 0.55 *Mt* at 0.057% Mo, and the Donggou deposit of 0.708 *Mt* at 0.097% Mo (Li et al., 2003, 2007; Mao et al., 2008). The host granitic porphyry stocks of the deposits are spatially related to the Heyu and Tianshanmiao batholiths. It is worthy to evaluate the link between porphyry Mo mineralization and the life span of host granitic porphyry stocks and batholith, and figure out the factors controlling the Mo enrichment.

Zircon is ubiquitous in granitic rocks and is resistant to hydrothermal alteration even at high temperatures (Valley et al., 1994). Zircon Hf and O isotopes and U/Pb ages can provide robust constraints on the origin and crystallization history of granites (Hawkesworth and Kemp, 2006; Kemp et al., 2007; Valley et al., 1994; Zhu et al., 2017). In this study, we carried out *in situ* U/Pb and Hf-O isotope analyses for zircon crystals from the Heyu batholith and related Nannihu and Shangfanggou ore-bearing granitic porphyries were carried out. On the basis of the new data set, combined with literature data, we discussed the crystallization history and possible sources of Late Mesozoic granites and factors controlling the Mo mineralization in the East Qinling orogenic belt.

2. Geological background

2.1. Tectonic outlines

The East Qinling orogenic belt is part of the Central China orogenic belt which is bounded by the North China Craton to the north and the Yangtze Block to the south. The Central China orogenic belt extends more than 4000 km from the West Kunlun orogenic belt in the west, through the Qilian, West Qinling, and East Qinling, to the Dabie-Sulu orogenic belt in the east (Dong and Santosh, 2016; Meng and Zhang, 2000; Wu and Zheng, 2013) (Fig. 1). The East Qinling orogenic belt consists of four terranes, from north to south, including the southern margin of the North China Craton, the North Qinling and the belts, and the northern margin of the Yangtze Block (Dong et al., 2011; Shi et al., 2013; Wu and Zheng, 2013).

The southern margin of the North China Craton is separated from the North Qinling belt by the Machaoying fault in the south. The southern margin of the North China Craton has a major period of crustal growth in Neoarchean (2.5–2.8 Ga) (Diwu et al., 2013; Wang and Zhang, 2016; Yang et al., 2009). The Taihua Group in the basement is overlain by Proterozoic volcanic and sedimentary sequences and is composed of Archean amphibolite- to granulite-facies metamorphic rocks and Paleoproterozoic TTG gneisses. Preserved magmatic zircons from amphibolite- to granulite-facies metamorphic rocks were dated to be 2.5–2.7 Ga with two-stage Hf model age (T_{DM}^2) of 3.0 to 3.2 Ga (Huang et al., 2010; Wang and Zhang, 2016), whereas those from the TTG gneisses have ages of 2.3–2.5 Ga and T_{DM}^2 of 2.6–3.2 Ga (Huang et al., 2012; Wang et al., 2012; Xu et al., 2009; Yu et al., 2013). The mafic to felsic volcanic rocks of the Xiong'er Group in the overlying sequences formed in 1.75–1.80 Ga (Cui et al., 2011; He et al., 2009; Wang et al., 2010b; Zhao et al., 2004).

The North Qinling is composed of a Mesoproterozoic basement and overlying Neoproterozoic to Paleozoic volcanic-sedimentary sequences. The Mesoproterozoic basement consists of gneiss, amphibolite and marble of the Qinling Group (Shi et al., 2009; Wan et al., 2011; Yang et al., 2010). The overlying Neoproterozoic sequence is mainly composed of the meta-basalts and meta-sedimentary rocks of the Kuanping Group (Diwu et al., 2010; Shi et al., 2009; Zhao et al., 2015). The Kuanping Group was the reworking products of the early Paleoproterozoic (~2.0–2.5 Ga) and the late Paleoproterozoic (~1.7 Ga) crust (Zhu et al., 2011). The overlying Paleozoic sequence is mainly composed of the meta-volcanic rocks and sedimentary rocks of the Erlangping Group.

The South Qinling consists of Paleoproterozoic to Neoproterozoic basement and overlying Sinian to Triassic sedimentary rocks (Meng and Zhang, 2000). The Paleoproterozoic basement is composed of dioritic-granitic gneisses of the Douling Complex. Preserved magmatic zircons from the gneisses were dated to be 2.47–2.51 Ga with T_{DM}^2 of 2.95–3.30 Ga (Hu et al., 2013). Neoproterozoic basement is composed of metamorphosed volcanic-sedimentary sequences of the Wudang Group. The South Qinling experienced multistage crustal growth and reworking in two periods of 1.5–1.8 Ga and 2.3–2.5 Ga (Hu et al., 2016; Ling et al., 2010; Zhang et al., 2016; Zhu et al., 2009, 2014).

The northern margin of the Yangtze Block is composed of Neoarchean to Paleoproterozoic basement and overlying Mesoproterozoic to Paleozoic sequences. The basement consists of TTG gneiss, migmatite, amphibolite and sedimentary rocks of the Kongling Group (Li et al., 2014; Ling, 1996; Yin et al., 2013). Overlying sequences consist of Meso- and Neo-proterozoic greenschist facies metamorphosed mafic and granitoid intrusions, and the Sinian to middle Triassic clastic-limestone (Dong and Santosh, 2016). The northern margin of the Yangtze Block experienced an important period of crust growth in Neoproterozoic (Liu et al., 2008; Wang et al., 2010a, 2013a; Yang et al., 2016; Zhao et al., 2011).

2.2. Late Mesozoic magmatism related to Mo mineralization in the East Qinling

The East Qinling orogenic belt experienced five stages of magmatism in Mesoproterozoic, Neoproterozoic, Paleozoic, the Early Mesozoic and Late Mesozoic (e.g., Bao et al., 2008, 2015; Dong et al., 2016; Wang et al., 2013c; Zeng et al., 2013). Major Mo mineralization is temporally associated with Late Mesozoic granitic magmatism in the belt (e.g., Bao et al., 2017; Li and Pirajno, 2017; Mao et al., 2011), forming giant porphyry Mo deposits including Nannihu, Shangfanggou, Yuchiling and Donggou. The host granitic porphyry stocks of the Nannihu, Shangfanggou and Yuchiling deposits are spatially and temporally associated with the Heyu batholith, whereas the granitic porphyry stock hosting the Donggou deposit is associated with the Taishanmiao batholith.

2.2.1. Heyu batholith and related granitic porphyry stocks

The Heyu batholith has an outcrop area of ~784 km^2 and is the largest Late Mesozoic granitic body in the East Qinling orogenic belt (Fig. 2). It intrudes the metamorphic rocks of the Taihua Group and the volcanic rocks of the Xiong'er Group. Zircon grains from the batholith have $^{206}Pb/^{238}U$ ages of 150–134 Ma (Bao et al., 2014; Gao et al., 2010, 2009; Li et al., 2012; Zhu et al., 2013). The central part of the batholith is capped with rhyolite and andesite of the Xiong'er Group. The batholith is composed of medium- to coarse-grained biotite monzogranite in the central part and coarse-grained to pegmatitic biotite monzogranite

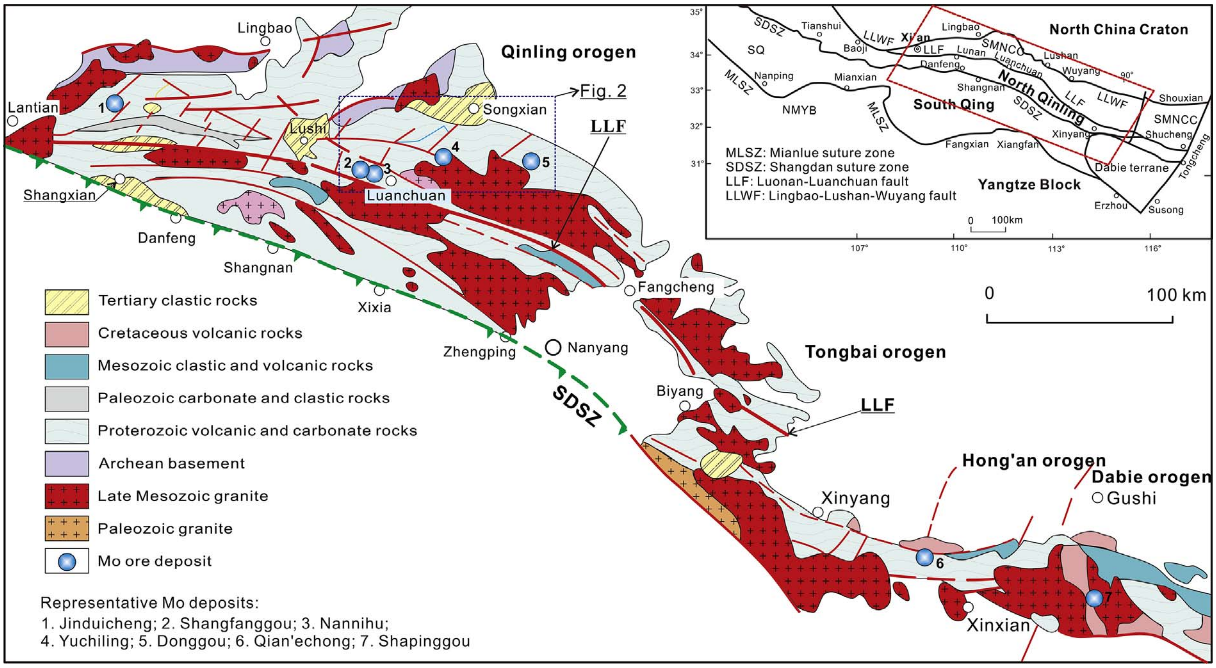

Fig. 1. A simplified geological map showing the distribution of Late Mesozoic granite plutons and major Mo deposits in the Qinling-Dabie orogenic belt (modified after Luo et al., 1991).

in the margin. However, the composition and texture of the rocks are transitional from the central part to margin. Coarse-grained and pegmatitic biotite monzogranite contain 20–40% K-feldspar phenocryst with grain size ranging from 4 × 6 cm to 8 × 12 cm. Medium- and coarse-grained biotite monzogranite contain 1–15% phenocrysts, which are mainly euhedral orthoclase and perthite with grain size from 0.8 × 1.0 cm to 1.5 × 2.5 cm.

Extrusive lobes of the Heyu batholith intrude the Neoproterozoic Luanchuan Group, forming a number of granitic porphyry stocks (Bao et al., 2014; Wang et al., 2006), with zircon $^{206}Pb/^{238}U$ ages of 150–134 Ma (Bao et al., 2014; Cheng et al., 2013; Li et al., 2015, 2013a; Wang et al., 2016b; Xiang et al., 2012). Ore-bearing granitic porphyry stocks are commonly small with outcrop areas less than 0.1 km^2. They are mainly composed of porphyritic biotite monzogranite and syenogranite with 5–50% phenocrysts. The phenocrysts include quartz, K-feldspar and plagioclase and show micrographic texture. Accessory minerals include apatite, magnetite, titanite, sphene, monazite, zircon and fluorite.

Ore bodies of the Nannihu and Shangfanggou deposits are hosted in granitic porphyry stocks and hornfels and skarn around the stocks. Major ore types include disseminated and veinlet-like ores. The ores are composed of molybdenite, sheelite, magnetite, pyrite, pyrrhotite and chalcopyrite, with minor sphalerite. Gangue minerals include quartz, garnet, diopside, fluorite and calcite. Molybdenite occurs as thin flakes in ores.

Ore bodies of the Yuchiling deposit are mainly hosted in the granitic porphyry, and locally in the cryptoexplosive breccia and adjacent monzogranite of the Heyu batholith. Major ore types include veinlet,

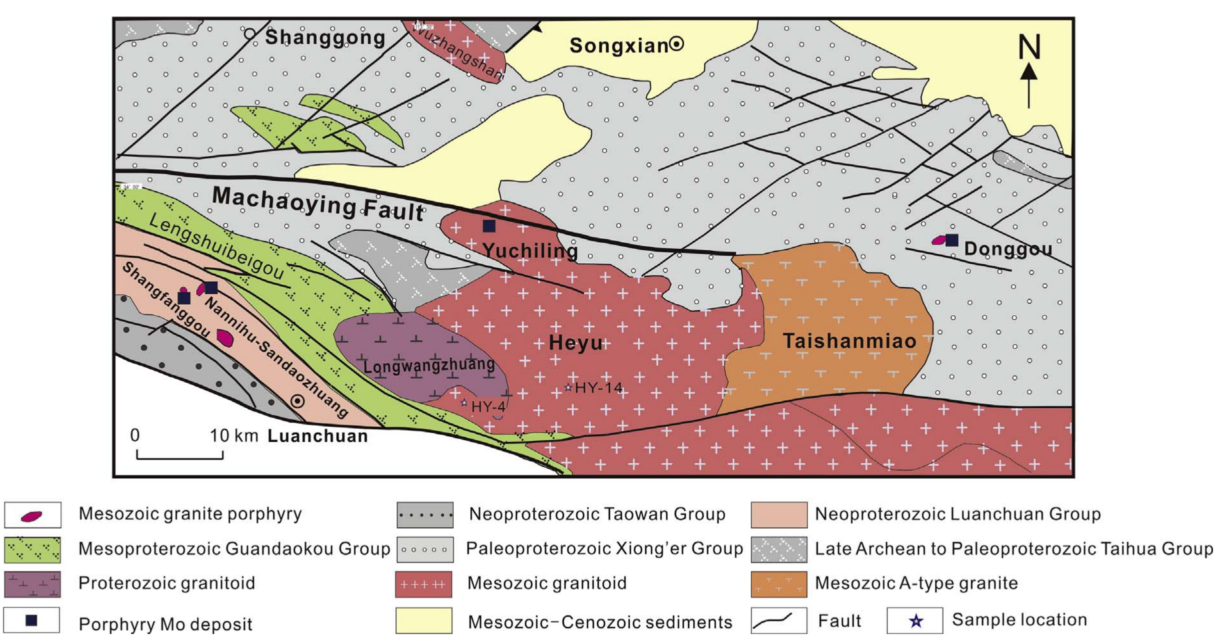

Fig. 2. A simplified geological map showing the distribution of the Heyu and Taishanmiao batholiths and related granitic porphyry stocks in the East Qinling orogenic belt.

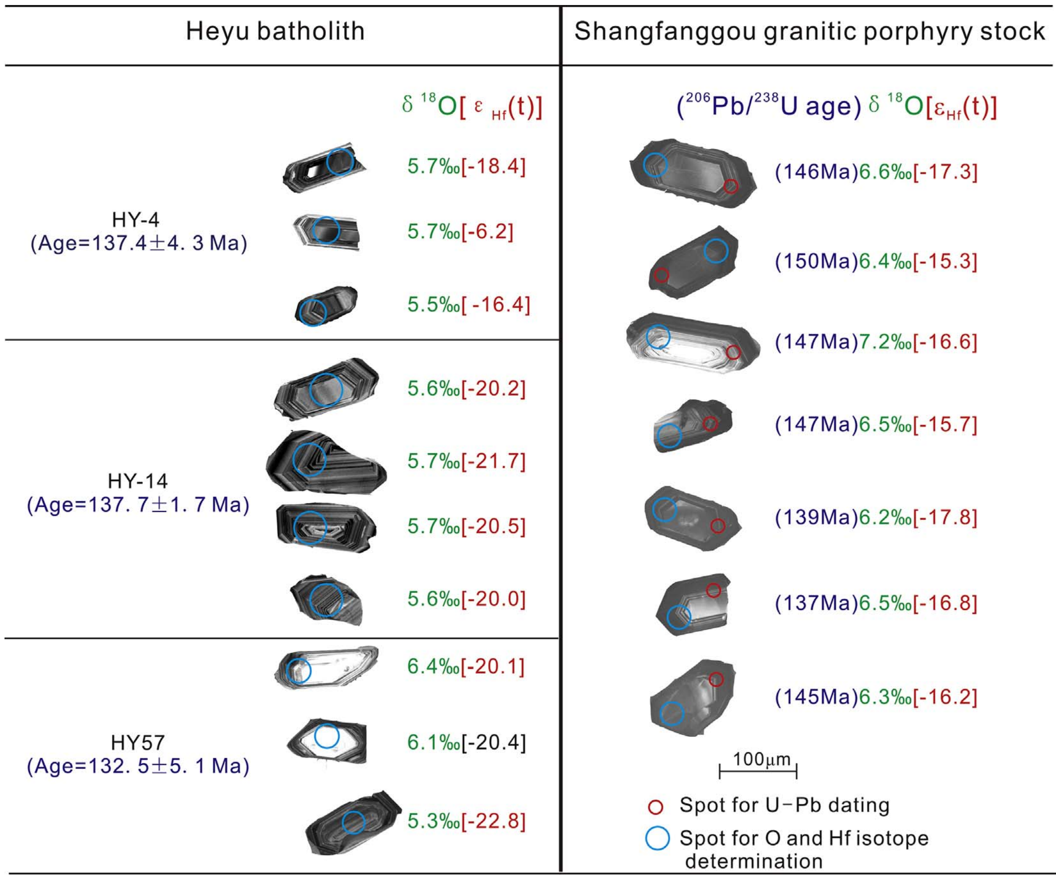

Fig. 3. CL images, U/Pb ages and O-Hf isotopic compositions for zircon grains from the Heyu batholith and Shangfanggou granitic porphyry stock.

disseminated and breccia ores. The ores are mainly composed of molybdenite and pyrite, chalcopyrite, galena and scheelite. Gangue minerals include K-feldspar, plagioclase, and quartz, minor sericite, muscovite, biotite, fluorite, and chlorite. Molybdenite occur as flake and lamellate in the veinlet and disseminated ores, or films in breccia ores.

Molybdenite from the Nannihu and Shangfanggou deposits have Re-Os model ages ranging from 139.3 ± 2.3 to 146.5 ± 2.3 Ma and 141.8 ± 2.1 to 145.4 ± 2.0 Ma, respectively, whereas molybdenite Re-Os model ages for the Yuchiling deposit range from 134.3 ± 2.0 to 141.8 ± 1.6 Ma (Li et al., 2013a; Mao et al., 2008; Xiang et al., 2012; Zhang et al., 2014b).

2.2.2. *Taishanmiao batholith and related granitic porphyry stocks*

The Taishanmiao batholith outcrops in an area of 290 km^2 (Gao et al., 2014; Ye et al., 2008b). Zircons from the batholith have $^{238}U/^{204}Pb$ ages ranging from 125 ± 1 to 113 ± 1 Ma (Gao et al., 2014; Wang et al., 2016a; Ye et al., 2008b). A branch of the batholith extends 7 km to the northeast, forming a granitic porphyry stock with an outcrop area of 0.01 km^2 that hosts the Donggou Mo deposit (e.g., Dai et al., 2009; Ye et al., 2008b). Zircons from the stock have $^{206}Pb/^{238}U$ ages ranging from 118 ± 1 to 112 ± 1 Ma (Dai et al., 2009; Gao et al., 2014; Wang et al., 2016a; Ye et al., 2008b). The ore bodies of the deposit occur in the contact zone between the stock and the volcanic rocks of the Xiong'er Group.

The Taishanmiao batholith consists of fine- to coarse-grained syenogranite in the southern part which changes gradationally to the fine-grained porphyritic syenogranite in the northern part. Porphyritic syenogranite dikes intrude the central and southern part of the batholith. Syenogranite and porphyritic syenogranite have similar mineral assemblages. Syenogranite shows equigranular texture and is composed of 45–65% K-feldspar, 10–15% plagioclase, 25–30% quartz and 2% biotite. Porphyritic syenogranite contains ~40% phenocrysts and ~60% groundmass. The phenocrysts include quartz, K-feldspar and plagioclase. The groundmass is composed of subhedral perthite, plagioclase and quartz.

Ore-bearing granitic porphyry shows porphyritic texture and is composed of ~10% phenocrysts and ~90% groundmass. The phenocrysts include quartz and perthite. Groundmass is composed of perthite, quartz, plagioclase and minor biotite. Accessory minerals include magnetite, anatase, sphene, rutile and zircon.

Major ore types of the Donggou deposit include veinlet and disseminated ores. Ore minerals include molybdenite with minor pyrite, chalcopyrite, galena, sphalerite, and scheelite. Gangue minerals are mainly quartz, alkali-feldspar, plagioclase, biotite and minor chlorite, epidote, sericite, and fluorite. Molybdenite in the veinlet and disseminated ores appears as subhedral flakes and bent scales. Molybdenite from the ores yielded the Re-Os model ages of 117.5 ± 0.8 to 115.5 ± 1.7 Ma (Li et al., 2017; Ye et al., 2008a).

3. Analytical methods

Zircon grains were separated from fresh or weakly altered rock samples that were collected from the Heyu batholith and the Nannihu and Shangfanggou granitic porphyry stocks. Zircon grains were separated using conventional heavy liquid and magnetic techniques, and purified by handpicking under a binocular microscope. They were mounted in epoxy resin, then polished to expose the grain centers and coated by gold. Transmitted and reflected light micrographs as well as cathodoluminescence (CL) images were obtained for the polished zircon grains in order to reveal their internal structure and external morphology, and guide the selection of potential analytical spots for oxygen, U/Pb, and Lu-Hf isotopic analyses. The CL images were made using a JEOL JXA-8100 electron microprobe equipped with Gatan

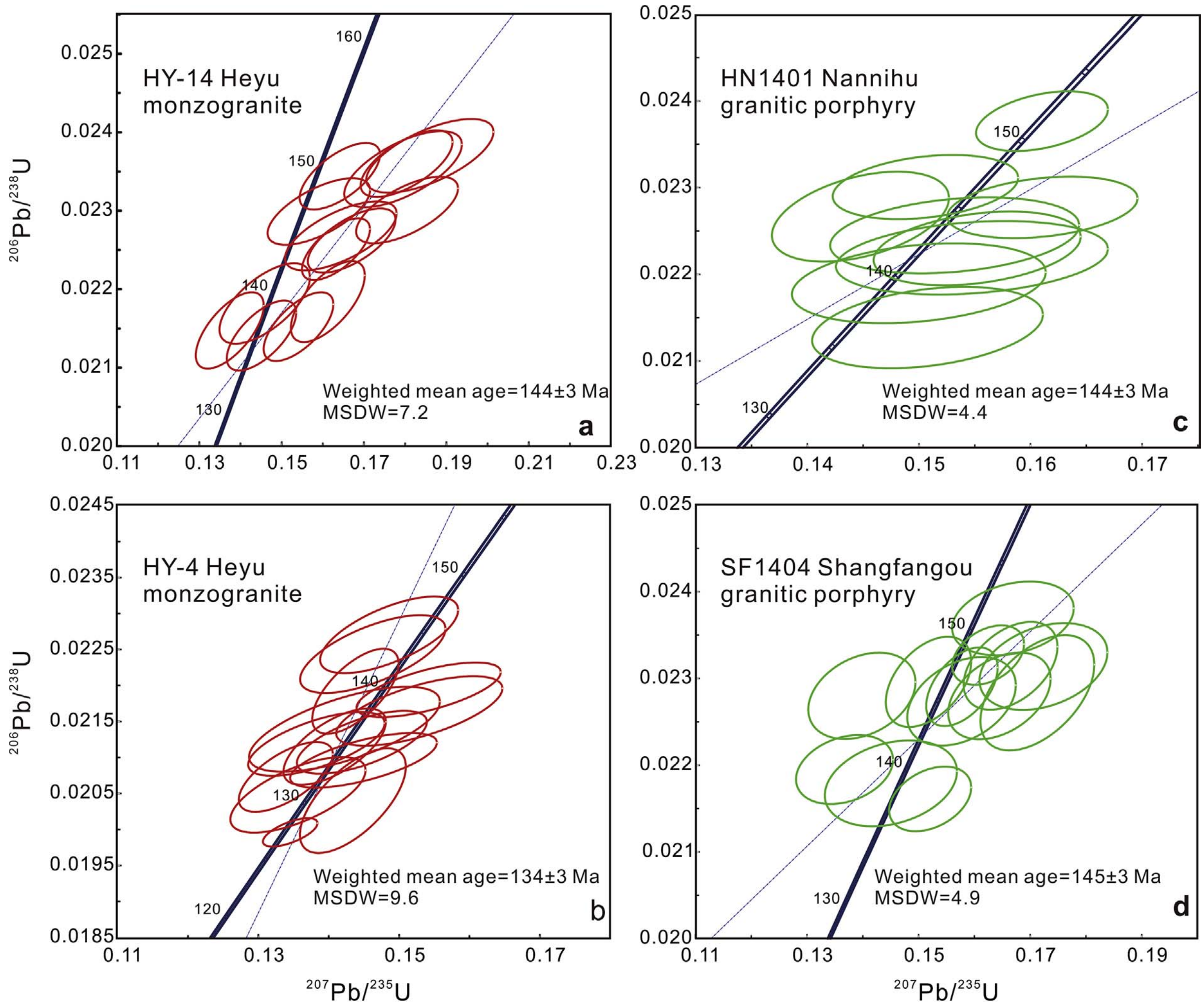

Fig. 4. U/Pb Concordia for zircon grains from the Heyu batholith (a and b) and Nannihu (c) and Shangfanggou (d) granitic porphyry stocks (data point error ellipses are 2σ).

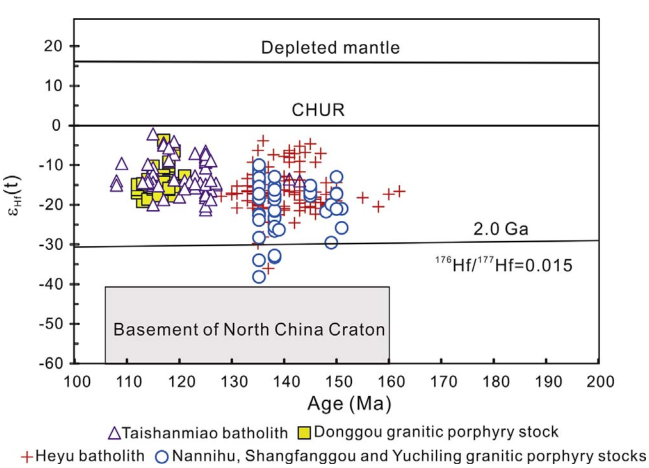

Fig. 5. Plot of U/Pb age versus $\varepsilon_{Hf}(t)$ for the zircon from the Heyu and Taishanmiao batholiths and coeval granitic porphyry stocks (Data from this study and Bao et al., 2014; Cheng et al., 2013; Dai et al., 2009; Gao et al., 2014; Li et al., 2012; Wang et al., 2016a; Yang et al., 2013a).

Mono CL3 system at the Guangzhou Institute of Geochemistry, Chinese Academy of Sciences (GIGCAS).

Most zircon grains in this study are clear, colorless, and euhedral. Only magmatic zircon crystals showing oscillatory zoning without inherited cores in CL images were selected for the analyses of U/Pb ages, and O and Lu-Hf isotopes.

3.1. Zircon U/Pb age analyses

Zircon grains were dated using an Agilent 7500a ICP-MS coupled with a Resonetics RESOlution M-50 193 nm laser-ablation system in GIGCAS. Details on operation conditions for the laser ablation system and the ICP-MS instrument and data processing are described by (Li et al., 2000; Liang et al., 1999). All analyses were carried out at an energy of 80 mJ, with a beam diameter of 31 μm and a repetition rate of 10 Hz. Helium was used as carrier gas to enhance the transportation efficiency of the ablated material. A TEMORA 1 (417 Ma) sample was used as zircon standard (Black et al., 2003). Integration of background and analytical signals, and time-drift correction and quantitative calibration for trace elements, were undertaken by using the GLITTER 4.0 algorithm (Macquarie University). The analytical data were reduced, calculated, and plotted by using the Isoplot 3.0 programs of Ludwig (2003).

3.2. Zircon O isotope analyses

Zircon O isotopic compositions were analyzed by using the Cameca IMS 1280HR ion microprobe in GIGCAS. The detailed analytical procedures were similar to those described by Li et al. (2010a). The measured oxygen isotopic data were corrected for instrumental mass fractionation by using the Penglai ($\delta^{18}O_{VSMOW}$ = 5.3‰) zircon standards (Li et al., 2010b). The internal precision of a single analysis generally

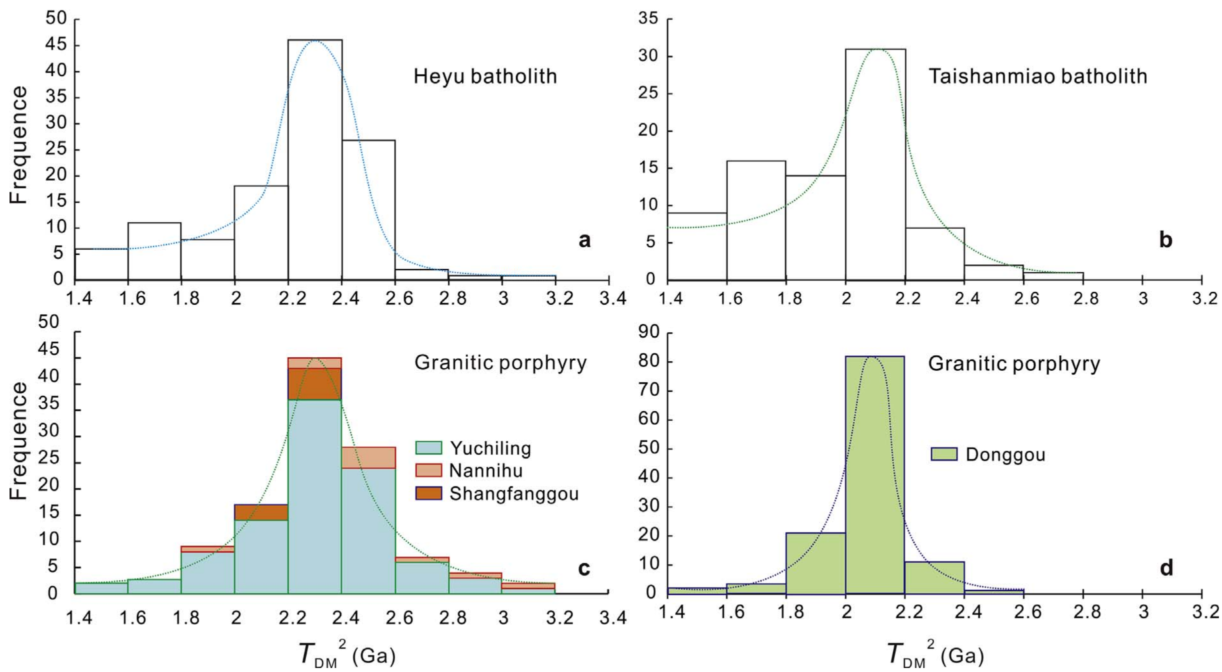

Fig. 6. Histograms of two-stage Hf model ages for the zircons from the Heyu (a) and Taishanmiao (b) batholiths and coeval granitic porphyry stocks (c and d) (Data from this study and Bao et al., 2014; Cheng et al., 2013; Dai et al., 2009; Gao et al., 2014; Li et al., 2012; Wang et al., 2016a; Yang et al., 2013a).

was better than 0.20‰ (1σ) for the $^{18}O/^{16}O$ ratio. The external precision, measured by the reproducibility of repeated analyses of Penglai and Qinghu standards (Li et al., 2013b), is 0.32‰ (2σ, n = 20). The instrumental mass fractionation factor is corrected using 91,500 zircon standard with $\delta^{18}O_{VSMOW}$ = 9.9‰ (Wiedenbeck et al., 2004).

3.3. Zircon Lu-Hf isotope analyses

Zircon Lu-Hf isotopic compositions were analyzed using a Neptune Plus multiple-collector inductively coupled plasma mass spectrometer with RESOlution M-50-LR laser ablation (ArF-excimer 193-nm wavelength) in GIGCAS. The Penglai zircon grains were selected as reference material (Li et al., 2010b) with the precision of 0.282882 ± 0.000006 (2σ, N = 56). The analytical procedures follow those described by Wu et al. (2006b). In the experiment, helium was used as the abrasion material carrier gas, and the diameter of the laser beam spot is 33 μm with energy of 80 mJ and repeat frequency of 8 Hz.

4. Results

4.1. Zircon U/Pb ages

Zircon grains from the Heyu batholith have concordant U/Pb ages scattered in a range of more than ~10 m.y. on the Concordia (Fig. 4a and b). The grains from a pegmatitic biotite monzogranite sample that was collected in the margin of the batholith (sample HY-4) have concordant $^{206}Pb/^{238}U$ ages ranging from 128 to 156 Ma, which yield a weighted mean $^{206}Pb/^{238}U$ age of 134 ± 3 Ma (MSWD = 9.6). The grains from a coarse-grained biotite monzogranite sample collected in the central part of the batholith (sample HY-14) have concordant $^{206}Pb/^{238}U$ ages ranging from 132 to 158 Ma, which yield a weighted mean $^{206}Pb/^{238}U$ age of 144 ± 3 Ma (MSWD = 7.2).

Zircon grains from the granitic porphyry stocks that host the Nannihu and Shangfanggou deposits also have scattered ranges of U/Pb age (Fig. 4c and d, Table S1). The grains from a granitic porphyry sample of the Nannihu deposit (HN1401) have $^{206}Pb/^{238}U$ ages ranging from 136 to 151 Ma, with a weighted mean $^{206}Pb/^{238}U$ age of 144 ± 3 Ma (MSWD = 4.4). The grains from a granitic porphyry sample of the Shangfanggou deposit (SF1404) have $^{206}Pb/^{238}U$ ages ranging from 138 to 151 Ma, with a weighted mean $^{206}Pb/^{238}U$ age of 145 ± 3 Ma (MSWD = 4.9). The large age ranges for the Heyu batholith and Nannihu and Shangfanggou granitic porphyry stocks obtained in this study are consistent with those reported in the literature (e.g., Guo et al., 2009; Li et al., 2012; Zhu et al., 2013).

4.2. Zircon O isotopic compositions

Zircon grains from the Heyu batholith and the Shangfanggou ore-bearing granitic porphyry have $\delta^{18}O$ ranging from +5.0 to +8.7‰ (Fig. 3 and Table S2), and nearly 50% of the grains have $\delta^{18}O$ close to the mantle value of 5.3 ± 0.6‰ (Valley et al., 2005). The gains from the Heyu batholith have $\delta^{18}O$ varying from + 5.0 to + 8.6‰, whereas those from the Shangfanggou ore-bearing granitic porphyry have $\delta^{18}O$ ranging from +5.0 to +8.7‰, identical to those for the Heyu batholith (Fig. 3).

4.3. Zircon Lu-Hf isotopic compositions

Zircon grains from the Heyu batholith have $\varepsilon_{Hf}(t)$ values ranging from −52 to −3.8. Two-stage Hf model ages ($T_{DM}{}^2$) were calculated to be in a range from 1.4 to 3.4 Ga. Zircon grains from the Shangfanggou ore-bearing granitic porphyry have $\varepsilon_{Hf}(t)$ values ranging from −47 to −10, with calculated $T_{DM}{}^2$ from 1.8 to 3.3 Ga (Figs. 5, 6a, b and Table S3). Most zircons from the batholith and ore-bearing granitic porphyry have $\varepsilon_{Hf}(t)$ ranging from −10 to −30 and $T_{DM}{}^2$ from 1.6 to 2.5 Ga (Figs. 5 and 6).

Zircon grains from the Taishanmiao batholith have $\varepsilon_{Hf}(t)$ values ranging from −21 to −2.1, with calculated $T_{DM}{}^2$ from 1.3 to 2.5 Ga, whereas those from the Donggou ore-bearing granitic porphyry have $\varepsilon_{Hf}(t)$ from −19 to −3.8 and $T_{DM}{}^2$ from 1.4 to 2.3 Ga (Dai et al., 2009; Gao et al., 2015; Yang et al., 2013a) (Figs. 5, 6b and d). Overall, nearly 90% of zircon grains from the Taishanmiao batholith and Donggou ore-bearing granitic porphyry have $T_{DM}{}^2$ from 1.6 to 2.3 Ga (Fig. 6).

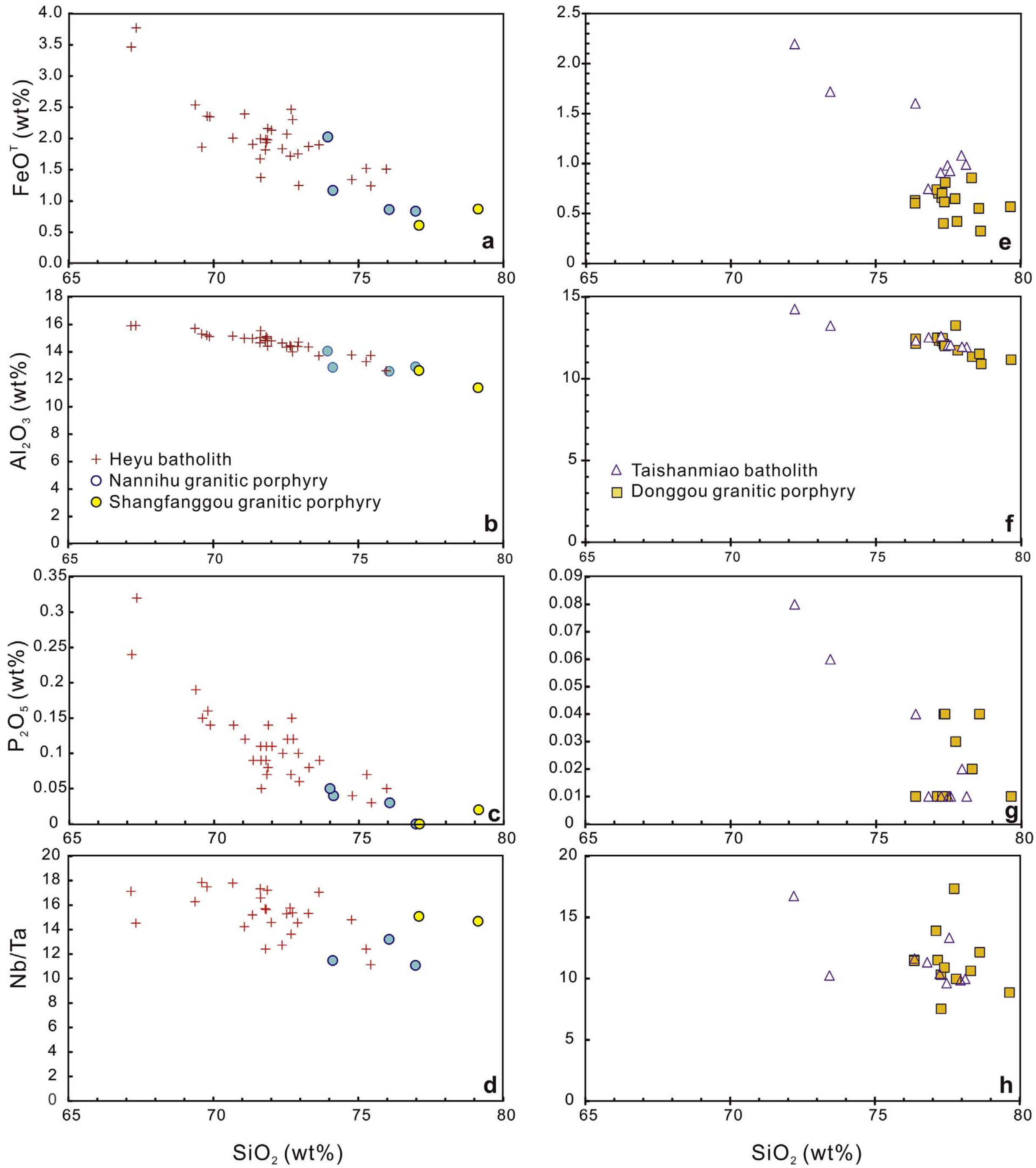

Fig. 7. Harker plots for the Late Mesozoic batholiths and coeval granitic porphyry stocks (Data from Bao et al., 2014; Dai et al., 2009; Gao et al., 2014; Yang et al., 2013a).

5. Discussion

5.1. A genetic link between batholith and ore-bearing granitic porphyry stocks

Zircon grains from the Heyu batholith and Nannihu and Shangfanggou ore-bearing granitic porphyry stocks have similar, scattered ranges of $^{206}Pb/^{238}U$ ages, indicating that they are coeval and have similar history of crystallization. They also have similar $\varepsilon_{Hf}(t)$ values of −10 to −30 and T_{DM}^2 of 1.6 to 2.5 Ga (Figs. 5 and 6), indicating that the Heyu batholith and two ore-bearing granitic porphyry stocks are comagmatic in origin. Likewise, the Taishanmiao batholith and Donggou ore-bearing granitic porphyry stock have comparable ranges of $^{206}Pb/^{238}U$ ages, and $\varepsilon_{Hf}(t)$ and T_{DM}^2 ages (Dai et al., 2009; Gao et al., 2014; Wang et al., 2016a; Yang et al., 2013a; Ye et al., 2008b) (Figs. 5b, 6c and d). Most zircon grains from the batholith and stock have $\varepsilon_{Hf}(t)$ values of −10 to −20 and T_{DM}^2 of 1.6 to 2.2 Ga, indicating that the Taishanmiao batholith and Donggou granitic porphyry stock are also comagmatic in origin.

A consanguinity between batholith and coeval ore-bearing granitic porphyry is also supported by similar Sm-Nd isotopic compositions of the rocks. The rocks from the Heyu batholith have $\varepsilon_{Nd}(t)$ values ranging from −18 to −10, with calculated two-stage Nd model ages in a range of 1.9–2.4 Ga. The rocks from the Nannihu and Shangfanggou ore-bearing granitic porphyry stocks have $\varepsilon_{Nd}(t)$ values of −16 to −13 and two-stage Nd model ages of 2.0–2.3 Ga (Bao et al., 2014; Gao et al., 2010). Likewise, the rocks from the Taishanmiao batholith have $\varepsilon_{Nd}(t)$ values of −16 to −10 and two-stage Nd model ages of 1.8 to 2.3 Ga,

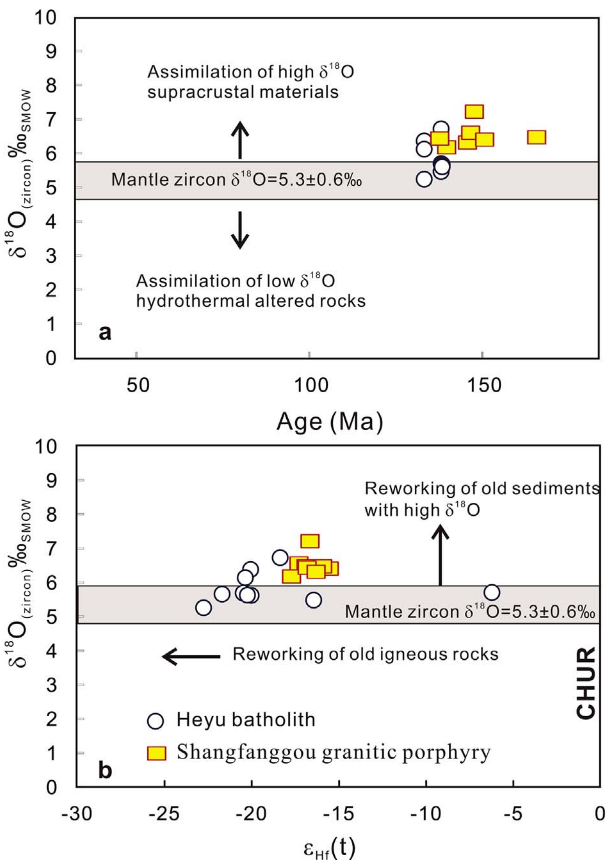

Fig. 8. Plots of $\delta^{18}O_{(Zircon)}$‰ versus age (a) and $\varepsilon_{Hf}(t)$ (b) for the zircon from the Heyu batholith and Shangfanggou granitic porphyry stock.

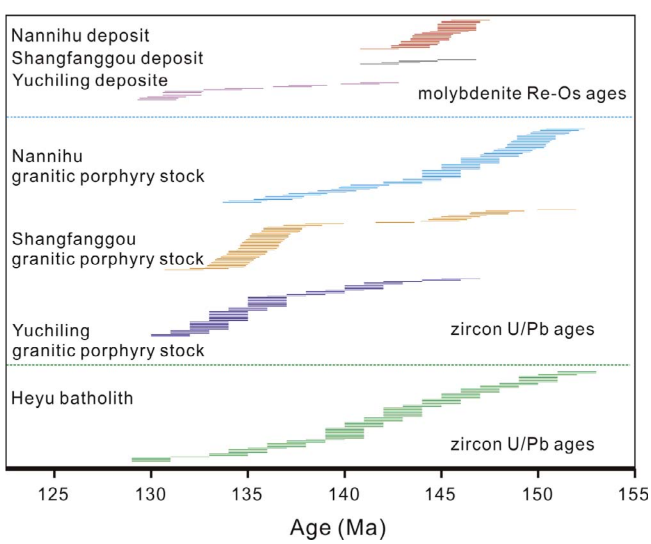

Fig. 9. Age spectra of zircon U/Pb ages for the Heyu batholith, and Nannihu, Shangfanggou and Yuchiling granitic porphyry stocks and Re-Os model ages of Mo deposits (Data from Bao et al., 2014; Li et al., 2003, 2005, 2012, 2013a; Xiang et al., 2012; Zhang et al., 2014ba).

similar to $\varepsilon_{Nd}(t)$ of −17 to −13 and two-stage model ages of 2.0 to 2.4 Ga for the Donggou ore-bearing granitic porphyry stock (Dai et al., 2009; Gao et al., 2014; Yang et al., 2013a).

The rocks of the Heyu batholith and Nannihu and Shangfanggou ore-bearing granitic porphyry stocks are calc-alkaline and metaluminous to peraluminous, whereas those from the Taishanmiao batholith and Donggou ore-bearing granitic porphyry stock are high-K calc-

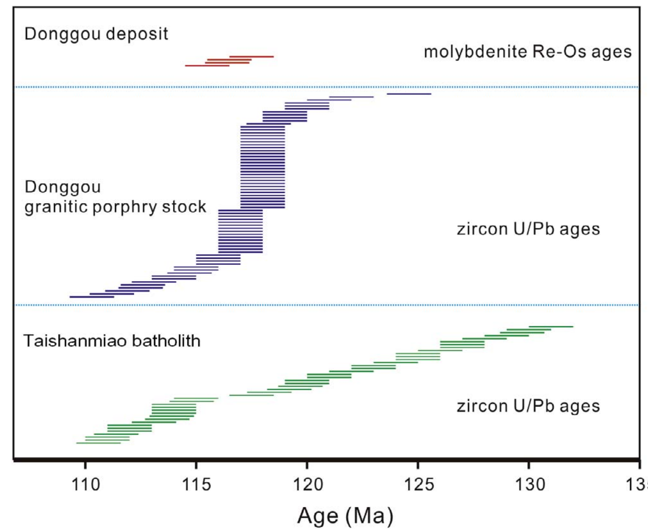

Fig. 10. Age spectra of zircon U/Pb ages for the Taishanmiao batholith and Donggou granitic porphyry stock and Re-Os model ages of Mo deposit (Data from Gao et al., 2014; Li et al., 2017; Yang et al., 2013a; Ye et al., 2008a, 2008b).

alkaline and peraluminous (Bao et al., 2014; Gao et al., 2010, 2014; Wang et al., 2016a; Yang et al., 2013a; Zhu et al., 2013). The samples from two batholiths and ore-bearing granitic porphyry stocks show linear trends of major oxides against SiO_2 on the Harker plots (Fig. 7). The samples from ore-bearing granitic porphyry stocks overall have SiO_2 higher than the batholiths, indicating that the ore-bearing granitic porphyries may represent the evolved end-members of the batholiths.

5.2. A protracted crystallization history of batholith and ore-bearing granitic porphyry stocks

Zircon grains from the Heyu batholith and Nannihu and Shangfanggou ore-bearing granitic porphyry stocks have a range of concordant $^{206}Pb/^{238}U$ ages over 10 m.y. (Fig. 4), which is a common feature for the granitic plutons elsewhere in the East Qinling orogenic belt and the whole Qinling-Dabie orogenic belt (e.g., Bao et al., 2014; Dai et al., 2009; Guo et al., 2009; Han et al., 2013; Li et al., 2012; 2013a; Wang et al., 2016a; Ye et al., 2008a; Zhu et al., 2013). This may imply that both batholiths and granitic porphyries in the East Qinling orogenic belt were constructed by multiple pulses of magma emplacement (Figs. 9 and 10).

Incremental growth of granitic plutons has been eventually recognized in diverse scales and tectonic environments. Protracted zircon crystallization and incremental assembly are common features in granitic plutons (Claiborne et al., 2010; Coleman et al., 2004; Davis et al., 2012; Heinonen et al., 2016; Kaiser et al., 2017; Matzel et al., 2006; Miller, 2008; Miller et al., 2007, 2011; Rezeau et al., 2016; Walker et al., 2007; Wiedenbeck et al., 2004). The youngest zircon age was usually suggested to be a proxy for the crystallization age of a pluton (Schaltegger et al., 2009). However, age brackets based on individual magmatic zircon grains may be more informative, and a prolonged crystallization history recorded in zircon may indicate a long lifetime of the magma reservoir from which porphyries and ore fluids were extracted (von Quadt et al., 2011). Zircon U/Pb ages that are dispersed out of analytical error may have been resulted from high-temperature fluctuation in a long-lived magmatic system (Miller, 2008; Miller et al., 2007; Walker et al., 2007). The longevity of porphyry ore systems may reflect the multiple intrusions that intermittently replenished porphyry stocks and contributed to the formation of giant magmatic-hydrothermal ore deposits (Sillitoe and Mortensen, 2010; von Quadt et al., 2011). Therefore, protracted magmatism is probably a key prerequisite for porphyry deposits (Rezeau et al., 2016). In the East

Qinling orogenic belt, the Re-Os model ages of molybdenite of Mo deposits are consistent with the younger ends of the age brackets for each of the host ore-bearing granitic porphyry stocks, indicating that the Mo mineralization likely occur concurrently with the late-stage magmatism in different stocks. We therefore consider that a protracted history of the Late Mesozoic batholiths and granitic porphyries in the East Qinling orogenic belt is likely a key factor controlling the formation of giant porphyry Mo deposits in the belt.

5.3. Source rocks of Late Mesozoic granitic magmatism

The Late Mesozoic batholiths and ore-bearing granitic porphyry stocks in the East Qinling orogenic belt have whole-rock $\varepsilon_{Nd}(t)$ and zircon $\varepsilon_{Hf}(t)$ values significantly higher than that of the basement in the southern margin of the North China Craton (e.g., Wang et al., 2010b; Yu et al., 2013). Many researchers therefore considered that they were likely derived from remelting of the Taihua Group and Xiong'er Group with the input of depleted mantle and/or juvenile crust (e.g., Li et al., 2012, 2015; Zhu et al., 2010). However, the addition of juvenile crust into the HFSE-enriched crust will have little effect on the isotopic signature of the resultant magma (Kirkland et al., 2013). There are a few lines of evidence indicating that the lithospheric mantle beneath the North China Craton was isotopically enriched before ca. 110 Ma in the Late Mesozoic (e.g., Meng et al., 2015; Wu et al., 2006a; Xu et al., 2004; Zhang and Sun, 2002); the Mesozoic mafic dikes in the southern margin of the North China Craton are isotopically enriched (Wang et al., 2008a, 2008b), and ~148 Ma mafic dikes in the study area have $\varepsilon_{Nd}(t)$ values of −6.6 to −7.0 (Bao et al., 2014). The early Cretaceous calc-alkaline basalts and mafic dikes in the North China Craton have $^{87}Sr/^{86}Sr_i$ of 0.706 to 0.710, $\varepsilon_{Nd}(t)$ of −1.7 to −17.5 and $\varepsilon_{Hf}(t)$ of −18.0 to −2.8 (Meng et al., 2015; Zhang and Sun, 2002). If the whole-rock Nd isotopic compositions of Late Mesozoic granites in the southern margin of the North China Craton can be produced by the mixing of the mantle with ε_{Nd} of −7 and the basement of the Taihua and Xiong'er Group rocks with ε_{Nd} of −25 to −50, the proportion of the mantle will exceed that of the crust in the modeling (Diwu et al., 2013; Guo et al., 2009; Ni et al., 2012). This is actually impossible in terms of major oxide contents of the rocks. Therefore, it is unlikely that the Taihua and Xiong'er Group rocks are the source of the Late Mesozoic granites in the southern margin of the North China Craton in the East Qinling orogenic belt. On the contrary, Late Mesozoic granitic rocks have whole-rock Nd isotopic compositions and zircon Hf isotopic compositions similar to those for the subducted continental crust of the Yangtze Block (Lu et al., 2004). As the crust of the northern margin of the Yangtze Block grew predominantly in Neoproterozoic (Wang et al., 2013a; Yang et al., 2015, 2016; Zhang et al., 2016) and contains voluminous Neoproterozoic volcanic rocks (Dong et al., 2012), melting of the crust of the Yangtze Block may account for the low $\delta^{18}O$ (5.0–8.7‰), highly negative $\varepsilon_{Hf}(t)$ (−10 to −30) and old T_{DM}^2 (1.6–2.5 Ga) of the Late Mesozoic granites in the southern margin of the North China Craton (Fig. 8). Therefore, it is likely that the Late Mesozoic granites in the southern margin of the North China Craton may have been derived from recycled, subducted continental crust of the Yangtze Block (Bao et al., 2014, 2017).

The Yangtze Block consists of the lower Cambrian Mo-rich black shales that contain > 100 ppm Mo (Jiang et al., 2009; Xu and Li, 2015; Xu et al., 2011). The Yangtze Block was supposed to have subducted underneath the southern margin of the North China Craton in Triassic. We therefore consider that melting of the Mo-rich black shales could activate and release Mo, forming extensive Mo mineralization hosted in Late Mesozoic granites in the East Qinling porphyry Mo belt (Bao et al., 2009, 2014, 2017; Zhang et al., 2014a).

6. Conclusions

The Late Mesozoic batholiths and ore-bearing granitic porphyries in the southern margin of the North China Craton have a geochemical affinity to the crust of the northern margin of the Yangtze Block, indicative the involvement of subducted Mo-rich crustal materials of the northern margin of the Yangtze Block. The ore-bearing granitic porphyries and coeval batholiths were constructed through incremental assembly and have protracted history of crystallization over 10 m.y., which is crucial to the exsolution of magmatic hydrothermal fluids and extraction of ore metals.

Acknowledgements

This study is financially supported by the MOST project No. 2016YFC0600405 and NSFC grant No. 41372083. We are grateful to Christina Yan Wang and Hecai Niu for their constructive discussion and suggestions, and Jiangwei Han in the Henan Institute of Geological Survey for his assistance in the field work. Constructive comments and suggestions from three anonymous reviewers, Taiping Zhao (guest editor) and Mei-Fu Zhou (editor-in-chief), significantly improved the manuscript.

Appendix A. Supplementary material

Supplementary data associated with this article can be found, in the online version, at https://doi.org/10.1016/j.jseaes.2017.12.022.

References

Bao, Z.W., Wang, Q., Bai, G.D., Zhao, Z.H., Song, Y.W., Liu, X.M., 2008. Geochronology and geochemistry of the Fangcheng Neoproterozoic alkali-syenites in East Qinling orogen and its geodynamic implications. Chinese Sci Bull 53, 2050–2061.
Bao, Z.W., Zeng, Q.S., Zhao, T.P., Yuan, Z.L., 2009. Geochemistry and petrogenesis of the ore-related Nannihu and Shangfanggou granite porphyries from east Qinling belt and their constaints on the molybdenum mineralization. Acta Petrol Sin 25, 2523–2536 (in Chinese with English abstract).
Bao, Z.W., Wang, C.Y., Zhao, T.P., Li, C.J., Gao, X.Y., 2014. Petrogenesis of the Mesozoic granites and Mo mineralization of the Luanchuan ore field in the East Qinling Mo mineralization belt, Central China. Ore Geol. Rev. 57, 132–153.
Bao, Z.W., Wang, C.Y., Zeng, L.J., Sun, W.D., Yao, J.M., 2015. Slab break-off model for the Triassic syn-collisional granites in the Qinling orogenic belt, Central China: Zircon U-Pb age and Hf isotope constraints. Int. Geol. Rev. 57, 492–507.
Bao, Z.W., Sun, W.D., Zartman, R.E., Yao, J.M., Gao, X.Y., 2017. Recycling of subducted upper continental crust: constraints on the extensive molybdenum mineralization in the Qinling-Dabie orogen. Ore Geol. Rev. 81, 451–465.
Black, L.P., Kamo, S.L., Allen, C.M., Aleinikoff, J.N., Davis, D.W., Korsch, R.J., Foudoulis, C., 2003. TEMORA 1: a new zircon standard for Phanerozoic U-Pb geochronology. Chem. Geol. 200, 155–170.
Chen, H.J., Chen, Y.J., Zhang, J., Chen, X.Z., Zhang, H.D., 2013. Zircon U-Pb ages and Hf isotope characteristics of the ore-bearing intrusion from the Shapinggou molybdenum deposit, Jinzhai County, Anhui Province. Acta Petrol Sin 29, 131–145 (in Chinese with English abstract).
Chen, W., Xu, Z.W., Qiu, W.H., Li, C., Yu, Y., Wang, H., Su, Y., 2015. Petrogenesis of the Yaochong granite and Mo depsoit, Western Dabie orogen, eastern-central China: Constraints from zircon U-Pb and molybdenite Re-Os ages, whole-rock geochemistry and Sr-Nd-Pb-Hf isotopes. J. Asian Earth Sci. 103, 198–211.
Cheng, Z.Y., Hu, J., Jiang, S.Y., Zhang, Z.Z., Dai, B.Z., Xiao, E., Wang, Y.F., 2013. Zircon U-Pb dating and Hf isotopes of the granites related to Yuchiling Mo deposit in Songxian County and their constraints on the metallogenetic age. Geol. J. China Univ. 19, 403–414 (in Chinese with English abstract).
Claiborne, L.L., Miller, C.F., Wooden, J.L., 2010. Trace element composition of igneous zircon: a thermal and compositional record of the accumulation and evolution of a large silicic batholith, Spirit Mountain, Nevada. Contrib. Miner. Petr. 160, 511–531.
Coleman, D.S., Gray, W., Glazner, A.F., 2004. Rethinking the emplacement and evolution of zoned plutons: Geochronologic evidence for incremental assembly of the Tuolumne Intrusive Suite, California. Geology 32, 433–436.
Coleman, D.S., Mills, R.D., Zimmerer, M.J., 2016. The pace of plutonism. Elements 12, 97–102.
Cui, M.L., Zhang, B.L., Zhang, L.C., 2011. U-Pb dating of baddeleyite and zircon from the Shizhaigou diorite in the southern margin of North China Craton: Constrains on the timing and tectonic setting of the Paleoproterozoic Xiong'er group. Gondwana Res. 20, 184–193.
Dai, B.Z., Jiang, S.Y., Wang, X.L., 2009. Petrogenesis of the granitic porphyry related to the giant molybdenum deposit in Donggou, Henan province, China: Constraints from petrogeochemistry, zircon U-Pb chronology and Sr-Nd-Hf isotopes. Acta Petr. Sin. 25, 2889–2901 (in Chinese with English abstract).
Davis, J.W., Coleman, D.S., Gracely, J.T., Gaschnig, R., Stearns, M., 2012. Magma accumulation rates and thermal histories of plutons of the Sierra Nevada batholith, CA. Contrib. Miner. Petr. 163, 449–465.
Diwu, C.R., Sun, Y., Liu, L.A., Zhang, C.L., Wang, H.L., 2010. The disintegration of Kuanping group in North Qinling orogenic belts and Neo-proterozoic N-MORB. Acta

Petrol. Sin. 26, 2025–2038 (in Chinese with English abstract).

Diwu, C.R., Sun, Y., Gao, J.F., Fan, L.G., 2013. Early Precambrian tectonothermal events of the North China Craton: Constraints from in situ detrital zircon U-Pb, Hf and O isotopic compositions in Tietonggou Formation. Chinese Sci. Bull. 58, 3760–3770.

Dong, Y.P., Santosh, M., 2016. Tectonic architecture and multiple orogeny of the Qinling Orogenic Belt, Central China. Gondwana Res. 29, 1–40.

Dong, Y.P., Liu, X.M., Santosh, M., Chen, Q., Zhang, X.N., Li, W., He, D.F., Zhang, G.W., 2012. Neoproterozoic accretionary tectonics along the northwestern margin of the Yangtze Block, China: constraints from zircon U-Pb geochronology and geochemistry. Precambr. Res. 196, 247–274.

Dong, Y.P., Genser, J., Neubauer, F., Zhang, G.W., Liu, X.M., Yang, Z., Heberer, B., 2011. U-Pb and Ar-40/Ar-39 geochronological constraints on the exhumation history of the North Qinling terrane, China. Gondwana Res. 19, 881–893.

Dong, Y.P., Yang, Z., Liu, X.M., Sun, S.S., Li, W., Cheng, B., Zhang, F.F., Zhang, X.N., He, D.F., Zhang, G.W., 2016. Mesozoic intracontinental orogeny in the Qinling Mountains, central China. Gondwana Res. 30, 144–158.

Farina, F., Stevens, G., Villaros, A., 2012. Multi-batch, incremental assembly of a dynamic magma chamber: the case of the Peninsula pluton granite (Cape Granite Suite, South Africa). Miner Petr. 106, 193–216.

Gao, Y., Mao, J.W., Ye, H.S., Meng, F., Li, Y.F., 2015. A review of the geological characteristics and geodynamic setting of the late Early Cretaceous molybdenum deposits in the East Qinling-Dabie molybdenum belt, East China. J. Asian Earth Sci. 108, 81–96.

Gao, X.Y., Zhao, T.P., Yuan, Z.L., Zhou, Y.Y., Gao, J.F., 2010. Geochemistry and petrogenesis of the Heyu batholith in the southern margin of the North China block. Acta Petrol. Sin. 26, 3485–3506 (in Chinese with English abstract).

Gao, X.Y., Zhao, T.P., Bao, Z.W., Yang, A.Y., 2014. Petrogenesis of the early Cretaceous intermediate and felsic intrusions at the southern margin of the North China Craton: Implications for crust-mantle interaction. Lithos 206, 65–78.

Guo, B., Zhu, L.M., Li, B., Gong, H.J., Wang, J.Q., 2009. Zircon U-Pb age and Hf isotope composition of the Huashan and Heyu granite plutons at the southern margin of North China Craton: implications for geodynamic setting. Acta Petrol. Sin. 25, 265–281 (in Chinese with English abstract).

Halter, W., Heinrich, C., Pettke, T., 2005. Magma evolution and the formation of porphyry Cu-Au ore fluids: evidence from silicate and sulfide melt inclusions. Miner. Deposita 39, 845–863.

Han, Y.G., Zhang, S.H., Pirajno, F., Zhou, X.W., Zhao, G.C., Qu, W.J., Liu, S.H., Zhang, J.M., Liang, H.B., Yang, K., 2013. U-Pb and Re-Os isotopic systematics and zircon Ce^{4+}/Ce^{3+} ratios in the Shiyaogou Mo deposit in eastern Qinling, central China: Insights into the oxidation state of granitoids and Mo (Au) mineralization. Ore Geol. Rev. 55, 29–47.

Hawkesworth, C.J., Kemp, A.I.S., 2006. Using hafnium and oxygen isotopes in zircons to unravel the record of crustal evolution. Chem. Geol. 226, 144–162.

He, Y.H., Zhao, G.C., Sun, M., Xia, X.P., 2009. SHRIMP and LA-ICP-MS zircon geochronology of the Xiong'er volcanic rocks: implications for the Paleo-Mesoproterozoic evolution of the southern margin of the North China Craton. Precambr. Res. 168, 213–222.

Hedenquist, J.W., Lowenstern, J.B., 1994. The role of magmas in the formation of hydrothermal ore-deposits. Nature 370, 519–527.

Heinonen, A., Manttari, I., Ramo, O.T., Andersen, T., Larjamo, K., 2016. A priori evidence for zircon antecryst entrainment in megacrystic Proterozoic granites. Geology 44, 227–230.

Hu, J., Liu, X.C., Chen, L.Y., Qu, W., Li, H.K., Geng, J.Z., 2013. A ∼ 2.5 Ga magmatic event at the northern margin of the Yangtze craton: evidence from U-Pb dating and Hf isotope analysis of zircons from the douling complex in the South Qinling orogen. Chinese Sci Bull 58, 3564–3579.

Hu, F.Y., Liu, S.W., Santosh, M., Deng, Z.B., Wang, W., Zhang, W.Y., Yan, M., 2016. Chronology and tectonic implications of Neoproterozoic blocks in the South Qinling Orogenic Belt, Central China. Gondwana Res. 30, 24–47.

Huang, X.L., Niu, Y.L., Xu, Y.G., Yang, Q.J., Zhong, J.W., 2010. Geochemistry of TTG and TTG-like gneisses from Lushan-Taihua complex in the southern North China Craton: Implications for late Archean crustal accretion. Precambr. Res. 182, 43–56.

Huang, X.L., Wilde, S.A., Yang, Q.J., Zhong, J.W., 2012. Geochronology and petrogenesis of gray gneisses from the Taihua Complex at Xiong'er in the southern segment of the Trans-North China Orogen: Implications for tectonic transformation in the Early Paleoproterozoic. Lithos 134, 236–252.

Jiang, S.Y., Pi, D.H., Heubeck, C., Frimmel, H., Liu, Y.P., Deng, H.L., Ling, H.F., Yang, J.H., 2009. Early Cambrian ocean anoxia in South China. Nature 459, E5–E6.

Kaiser, J.F., de Silva, S., Schmitt, A.K., Economos, R., Sunagua, M., 2017. Million-year melt-presence in monotounous intermdiate magma for a volcanic-plutonic assemblage in the Central Andes: contastin historyies of crystal-rich and crystal-ppor super-sized silicic magmas. Earth Planet. Sci. Lett. 457, 73–86.

Kemp, A.I.S., Hawkesworth, C.J., Foster, G.L., Paterson, B.A., Woodhead, J.D., Hergt, J.M., Gray, C.M., Whitehouse, M.J., 2007. Magmatic and crustal differentiation history of granitic rocks from Hf-O isotopes in zircon. Science 315, 980–983.

Kirkland, C.L., Smithies, R.H., Woodhouse, A.J., Howard, H.M., Wingate, M.T.D., Belousova, E.A., Cliff, J.B., Murphy, R.C., Spaggiari, C.V., 2013. Constraints and deception in the isotopic record; the crustal evolution of the west Musgrave Province, central Australia. Gondwana Res. 23, 759–781.

Li, Z.K., Bi, S.J., Li, J.W., Zhang, W., Cooke, D.R., Selby, D., 2017. Distal Pb-Zn-Ag veins associated with the world-class Donggou porphyry Mo deposit, southern North China craton. Ore Geol. Rev. 82, 232–251.

Li, N., Chen, Y.J., Zhang, H., Zhao, T.P., Deng, X.H., Wang, Y., Ni, Z.Y., 2007. Molybdenum deposits in East Qinling. Earth Sci. Front. 14, 186–198 (in Chinese with English abstract).

Li, N., Chen, Y.J., Pirajno, F., Gong, H.J., Mao, S.D., Ni, Z.Y., 2012. LA-ICP-MS zircon U-Pb dating, trace element and Hf isotope geochemistry of the Heyu granite batholith, eastern Qinling, central China: implications for Mesozoic tectono-magmatic evolution. Lithos 142, 34–47.

Li, N., Chen, Y.J., Pirajno, F., Ni, Z.Y., 2013a. Timing of the Yuchiling giant porphyry Mo system, and implications for ore genesis. Miner. Deposita 48, 505–524.

Li, D., Han, J.W., Zhang, S.T., Yan, C.H., Cao, H.W., Song, Y.W., 2015. Temporal evolution of granitic magmas in the Luanchuan metallogenic belt, east Qinling Orogen, central China: implications for Mo metallogenesis. J. Asian Earth Sci. 111, 663–680.

Li, X.H., Liang, X.R., Sun, M., Liu, Y., Tu, X.L., 2000. Geochronology and geochemistry of single-grain zircons: simultaneous in-situ analysis of U-Pb age and trace elements by LAM-ICP-MS. Eur. J. Miner. 12, 1015–1024.

Li, L.M., Lin, S.F., Davis, D.W., Xiao, W.J., Xing, G.F., Yin, C.Q., 2014. Geochronology and geochemistry of igneous rocks from the Kongling terrane: implications for Mesoarchean to Paleoproterozoic crustal evolution of the Yangtze Block. Precambr. Res. 255, 30–47.

Li, X.H., Long, W.G., Li, Q.L., Liu, Y., Zheng, Y.F., Yang, Y.H., Chamberlain, K.R., Wan, D.F., Guo, C.H., Wang, X.C., Tao, H., 2010b. Penglai zircon megacrysts: a potential new working reference material for microbeam determination of Hf-O isotopes and U-Pb age. Geostand. Geoanal. Res. 34, 117–134.

Li, X.H., Li, W.X., Li, Q.L., Wang, X.C., Liu, Y., Yang, Y.H., 2010a. Petrogenesis and tectonic significance of the similar to 850 Ma Gangbian alkaline complex in South China: evidence from in situ zircon U-Pb dating, Hf-O isotopes and whole-rock geochemistry. Lithos 114, 1–15.

Li, Y.F., Mao, J.W., Bai, F.J., Li, J.P., He, Z.J., 2003. Re-Os isotopic dating of molybdenites in the Nannihu molybdenum (tungsten) orefield in the Eastern Qinling and its geological significance. Geol. Rev. 49, 652–659 (in Chinese with English abstract).

Li, Y.F., Mao, J.W., Bai, F.J., Guo, B.J., Wang, Z.G., 2005. Precise Re-Os dating of molybdenite from the East Qinling molybdenum belt in central China and its geodynamic implications. Miner. Deposit Res.: Meet. Glob. Challenge 1 and 2, 777–780.

Li, N., Pirajno, F., 2017. Early mesozoic mo mineralization in the Qinling orogen: an overview. Ore Geol. Rev. 81, 431–450.

Li, X.H., Tang, G.Q., Gong, B., Yang, Y.H., Hou, K.J., Hu, Z.C., Li, Q.L., Liu, Y., Li, W.X., 2013b. Qinghu zircon: a working reference for microbeam analysis of U-Pb age and Hf and O isotopes. Chinese Sci. Bull. 58, 4647–4654.

Liang, X.R., Li, X.H., Sun, M., Liu, Y., Tu, X.L., 1999. Simultaneously in-situ analysis of trace elements and U-Pb and Pb-Pb ages for single zircons by laser ablation microprobe-inductively coupled plasma mass spectrometry. Chem. Lett. 639–640.

Ling, W.L., 1996. Isotopic geochronology and crustal growth of Proterozoic basement along the northern margin of Yangtze Craton: 1. Houhe Group and Xixiang Group. Earth Sci.-J. China Univ. Geosci. 21, 491–494 (in Chinese with English abstract).

Ling, W.L., Duan, R.C., Liu, X.M., Cheng, J.P., Mao, X.W., Peng, L.H., Liu, Z.X., Yang, H.M., Ren, B.F., 2010. U-Pb dating of detrital zircons from the Wudangshan Group in the South Qinling and its geological significance. Chinese Sci. Bull. 55, 2440–2448.

Liu, X.M., Gao, S., Diwu, C.R., Ling, W.L., 2008. Precambrian crustal growth of Yangtze craton as revealed by detrital zircon studies. Am. J. Sci. 308, 421–468.

Liu, Q.Q., Shao, Y.J., Zhang, Z.H., Zhang, Y., Li, B., Zhang, C., 2015. Zircon U-Pb ages, Hf isotope characteristics and its implication of granite from Yaochong, Dabie orogen, China. Chinese J. Nonferrous Met. 25, 479–491 (in Chinese with English abstract).

Lu, F.X., Wang, C.Y., Zheng, J.P., 2004. Lithospheric composition and structure beneath the northern margin of the Qinling orogenic belt - On deep-seated xenoliths in Minggang region of Henan Province. Sci. China Ser. D 47, 13–22.

Ludwig, K.R., 2003. Users Manual for Isoplot 3.00: A Geochronological Toolkit for Microsoft Excel. Berkeley Geochronology Center, Berkeley.

Luo, M.J., Zhang, F.M., Dong, Q.Y., 1991. Molybdenum deposits in China. Hennan Science and Technology Press, Zhengzhou.

Mao, J.W., Xie, G.Q., Bierlein, F., Qu, W.J., Du, A.D., Ye, H.S., Pirajno, F., Li, H.M., Guo, B.J., Li, Y.F., Yang, Z.Q., 2008. Tectonic implications from Re-Os dating of Mesozoic molybdenum deposits in the East Qinling-Dabie orogenic belt. Geochim. Cosmochim. Acta 72, 4607–4626.

Mao, J.W., Pirajno, F., Xiang, J.F., Gao, J.J., Ye, H.S., Li, Y.F., Guo, B.J., 2011. Mesozoic molybdenum deposits in the east Qinling-Dabie orogenic belt: characteristics and tectonic settings. Ore Geol. Rev. 43, 264–293.

Matzel, J.E.P., Bowring, S.A., Miller, R.B., 2006. Time scales of pluton construction at differing crustal levels: Examples from the Mount Stuart and Tenpeak intrusions, North Cascades, Washington. Geol. Soc. Am. Bull. 118, 1412–1430.

Meng, F.X., Gao, S., Niu, Y.L., Liu, Y.S., Wang, X.R., 2015. Mesozoic-Cenozoic mantle evolution beneath the North China Craton: a new perspective from Hf-Nd isotopes of basalts. Gondwana Res. 27, 1574–1585.

Meng, Q.R., Zhang, G.W., 2000. Geologic framework and tectonic evolution of the Qinling orogen, central China. Tectonophysics 323, 183–196.

Miller, J.S., 2008. Assembling a pluton... one increment at a time. Geology 36, 511–512.

Miller, C.F., Furbish, D.J., Walker, B.A., Claiborne, L.L., Koteas, G.C., Bleick, H.A., Miller, J.S., 2011. Growth of plutons by incremental emplacement of sheets in crystal-rich host: evidence from Miocene intrusions of the Colorado River region, Nevada, USA. Tectonophysics 500, 65–77.

Miller, J.S., Matzel, J.E.P., Miller, C.F., Burgess, S.D., Miller, R.B., 2007. Zircon growth and recycling during the assembly of large, composite arc plutons. J. Volcanol. Geoth. Res. 167, 282–299.

Ni, Z.Y., Chen, Y.J., Li, N., Zhang, H., 2012. Pb-Sr-Nd isotope constraints on the fluid source of the Dahu Au-Mo deposit in Qinling Orogen, central China, and implication for Triassic tectonic setting. Ore Geol. Rev. 46, 60–67.

Pettke, T., Oberli, F., Heinrich, C.A., 2010. The magma and metal source of giant porphyry-type ore deposits, based on lead isotope microanalysis of individual fluid inclusions. Earth Planet Sci. Lett. 296, 267–277.

Rezeau, H., Moritz, R., Wotzlaw, J.F., Tayan, R., Melkonyan, R., Ulianov, A., Selby, D., d'Abzac, F.X., Stern, R.A., 2016. Temporal and genetic link between incremental

pluton assembly and pulsed porphyry Cu-Mo formation in accretionary orogens. Geology 44, 627–630.
Schaltegger, U., Brack, P., Ovtcharova, M., Peytcheva, I., Schoene, B., Stracke, A., Marocchi, M., Bargossi, G.M., 2009. Zircon and titanite recording 1.5 million years of magma accretion, crystallization and initial cooling in a composite pluton (southern Adamello batholith, northern Italy). Earth Planet Sci. Lett. 286, 208–218.
Shi, Y., Yu, J.H., Xu, X.S., Qiu, J.S., Chen, L.H., 2009. Geochronology and geochemistry of the Qinling Group in the eastern Qinling Orogen. Acta Petrol. Sin. 25, 2651–2670 (in Chinese with English abstract).
Shi, Y., Yu, J.H., Santosh, M., 2013. Tectonic evolution of the Qinling orogenic belt, Central China: new evidence from geochemical, zircon U-Pb geochronology and Hf isotopes. Precambr. Res. 231, 19–60.
Sillitoe, R.H., Mortensen, J.K., 2010. Longevity of porphyry copper formation at Quellaveco, Peru. Econ. Geol. 105, 1157–1162.
Valley, J.W., Chiarenzelli, J.R., Mclelland, J.M., 1994. Oxygen-isotope geochemistry of zircon. Earth Planet Sci. Lett. 126, 187–206.
Valley, J.W., Lackey, J.S., Cavosie, A.J., Clechenko, C.C., Spicuzza, M.J., Basei, M.A.S., Bindeman, I.N., Ferreira, V.P., Sial, A.N., King, E.M., Peck, W.H., Sinha, A.K., Wei, C.S., 2005. 4.4 billion years of crustal maturation: oxygen isotope ratios of magmatic zircon. Contrib. Miner. Petr. 150, 561–580.
von Quadt, A., Erni, M., Martinek, K., Moll, M., Peytcheva, I., Heinrich, C.A., 2011. Zircon crystallization and the lifetimes of ore-forming magmatic-hydrothermal systems. Geology 39, 731–734.
Walker, B.A., Miller, C.F., Claiborne, L.L., Wooden, J.L., Miller, J.S., 2007. Geology and geochronology of the Spirit Mountain batholith, southern Nevada: implications for timescales and physical processes of batholith construction. J. Volcanol. Geoth. Res. 167, 239–262.
Wan, Y.S., Liu, D.Y., Dong, C.Y., Yin, X.Y., 2011. SHRIMP zircon dating of meta-sedimentary rock from the Qinling Group in the north of Xixia, North Qinling Orogenic Belt: Constraints on complex histories of source region and timing of deposition and metamorphism. Acta Petrol. Sin. 27, 1172–1178 (in Chinese with English abstract).
Wang, C.M., Deng, J., Zhang, S.T., Ye, H.S., 2006. Endogentic metallogenic system of Nannihu Mo-W-Cu-Pb-Zn-Ag-Au ore-forming area. Geol. Sci. Technol. Inform. 25, 47–52 (in Chinese with English abstract).
Wang, C.M., Chen, L., Bagas, L., Lu, Y.J., He, X.Y., Lai, X.R., 2016a. Characterization and origin of the Taishanmiao aluminous A-type granites: implications for Early Cretaceous lithospheric thinning at the southern margin of the North China Craton. Int. J. Earth Sci. 105, 1563–1589.
Wang, L.J., Griffin, W.L., Yu, J.H., O'Reilly, S.Y., 2010a. Precambrian crustal evolution of the Yangtze Block tracked by detrital zircons from Neoproterozoic sedimentary rocks. Precambr. Res. 177, 131–144.
Wang, L.J., Griffin, W.L., Yu, J.H., O'Reilly, S.Y., 2013a. U-Pb and Lu-Hf isotopes in detrital zircon from Neoproterozoic sedimentary rocks in the northern Yangtze Block: Implications for Precambrian crustal evolution. Gondwana Res. 23, 1261–1272.
Wang, X.L., Jiang, S.Y., Dai, B.Z., 2010b. Melting of enriched Archean subcontinental lithospheric mantle: Evidence from the ca. 1760 Ma volcanic rocks of the Xiong'er Group, southern margin of the North China Craton. Precambr. Res. 182, 204–216.
Wang, A.D., Liu, Y.C., Gu, X.F., Hou, Z.H., Song, B., 2012. Late-Neoarchean magmatism and metamorphism at the southeastern margin of the North China Craton and their tectonic implications. Precambr. Res. 220, 65–79.
Wang, T.H., Mao, J.W., Wang, Y.B., 2008a. Research on SHRIMP U-Pb chronology in Xiaoqinling-Xiongr' shan area: the evidence of delamination of lithosphere in Qinling orogenic belt. Acta Petrol. Sin. 24, 1273–1287.
Wang, T.H., Mao, J.W., Xie, G.Q., Ye, A.W., Li, Z.Y., 2008b. Sr, Nd, Pb isotopic composition of the Meso-basic dykes in the Xiaoqinling-Xiong'ershan area, Henan province, central China and its tectonic significance. Acta Geol. Sin. 82, 1580–1591 (in Chinese with English abstract).
Wang, Q.S., Teng, J.W., Zhang, Y.Q., Wen, W., Hua, C.C., 2013b. Discussion on the special gravity field across the north part of middle Qinling Mt. Chinese J. Geophys.-Ch. 56, 792–798.
Wang, X.X., Wang, T., Zhang, C.L., 2013c. Neoproterozoic, Paleozoic, and Mesozoic granitoid magmatism in the Qinling Orogen, China: constraints on orogenic process. J. Asian Earth Sci. 72, 129–151.
Wang, X.X., Wang, T., Ke, C.H., Yang, Y., Li, J.B., Li, Y.H., Qi, Q.J., Lv, X.Q., 2015. Nd-Hf isotopic mapping of Late Mesozoic granitoids in the East Qinling orogen, central China: Constraint on the basements of terranes and distribution of Mo mineralization. J. Asian Earth Sci. 103, 169–183.
Wang, S., Ye, H.S., Yang, Y.Q., Zhang, X.K., Su, H.M., Yang, C.Y., 2016b. Zircon chronology, geochemistry and Hf isotope compositions of the Huoshenmiao pluton, western Henan. Earth Sci. 41, 293–316 (in Chinese with English abstract).
Wang, J.L., Zhang, H.F., 2016. Three period tectonic-magmatic events recorded in ancient granulite of the North China Craton. Acta Petrol. Sin. 32, 682–696 (in Chinese with English abstract).
Wiedenbeck, M., Hanchar, J.M., Peck, W.H., Sylvester, P., Valley, J., Whitehouse, M., Kronz, A., Morishita, Y., Nasdala, L., Fiebig, J., Franchi, I., Girard, J.P., Greenwood, R.C., Hinton, R., Kita, N., Mason, P.R.D., Norman, M., Ogasawara, M., Piccoli, R., Rhede, D., Satoh, H., Schulz-Dobrick, B., Skar, O., Spicuzza, M.J., Terada, K., Tindle, A., Togashi, S., Vennemann, T., Xie, Q., Zheng, Y.F., 2004. Further characterisation of the 91500 zircon crystal. Geostand. Geoanal. Res. 28, 9–39.
Wu, F.Y., Yang, Y.H., Xie, L.W., Yang, J.H., Xu, P., 2006b. Hf isotopic compositions of the standard zircons and baddeleyites used in U-Pb geochronology. Chem. Geol. 234, 105–126.
Wu, F.Y., Walker, R.J., Yang, Y.H., Yuan, H.L., Yang, J.H., 2006a. The chemical-temporal evolution of lithospheric mantle underlying the North China Craton. Geochim. Cosmochim. Acta 70, 5013–5034.
Wu, Y.B., Zheng, Y.F., 2013. Tectonic evolution of a composite collision orogen: an overview on the Qinling-Tongbai-Hong'an-Dabie-Sulu orogenic belt in central China. Gondwana Res. 23, 1402–1428.
Xiang, J.F., Mao, J.W., Pei, R.F., Ye, H.S., Wang, C.Y., Tian, Z.H., Wang, H.L., 2012. New geochronological data of granites and ores from the Nannihu-Sandaozhuang Mo (W) deposit. Geol. China 39, 458–473 (in Chinese with English abstract).
Xu, X.S., Griffin, W.L., Ma, X., O'Reilly, S.Y., He, Z.Y., Zhang, C.L., 2009. The Taihua group on the southern margin of the North China craton: further insights from U-Pb ages and Hf isotope compositions of zircons. Miner. Petrol. 97, 43–59.
Xu, L.G., Lehmann, B., Mao, J.W., Qu, W.J., Du, A.D., 2011. Re-Os age of polymetallic Ni-Mo-PGE-Au mineralizaiton in early Cambrian black shales of South China-A reassessment. Econ. Geol. 106, 511–522.
Xu, J., Li, Y.L., 2015. An SEM study of microfossils in the black shale of the lower cambrian niutitang formation, Southwest China: implications for the polymetallic sulfide mineralization. Ore Geol. Rev. 65, 811–820.
Xu, Y.G., Ma, J.L., Huang, X.L., Iizuka, Y., Chung, S.L., Wang, Y.B., Wu, X.Y., 2004. Early cretaceous gabbroic complex from Yinan, Shandong Province: petrogenesis and mantle domains beneath the North China Craton. Int. J. Earth Sci. 93, 1025–1041.
Yang, L., Chen, F.K., Yang, Y.Z., Li, S.Q., Zhu, X.Y., 2010. Zircon U-Pb ages of the Qinling group in Danfeng area: recording mesoproterozoic and neoproterozoic magmatism and early paleozoic metamorphism in the North Qinling terrain. Acta Petrol. Sin. 26, 1589–1603 (in Chinese with English abstract).
Yang, Y., Chen, Y.J., Zhang, J., Zhang, C., 2013b. Ore geology, fluid inclusions and four-stage hydrothermal mineralization of the Shangfanggou giant Mo-Fe deposit in Eastern Qinling, central China. Ore Geol. Rev. 55, 146–161.
Yang, L., Chen, F.K., Liu, B.X., Hu, Z.P., Qi, Y., Wu, J.D., He, J.F., Siebel, W., 2013a. Geochemistry and Sr-Nd-Pb-Hf isotopic composition of the Donggou Mo-bearing granite porphyry, Qinling orogenic belt, central China. Int. Geol. Rev. 55, 1261–1279.
Yang, J., Gao, S., Chen, C., Tang, Y.Y., Yuan, H.L., Gong, H.J., Xie, S.W., Wang, J.Q., 2009. Episodic crustal growth of North China as revealed by U-Pb age and Hf isotopes of detrital zircons from modern rivers. Geochim. Cosmochim. Acta 73, 2660–2673.
Yang, Y.N., Wang, X.C., Li, Q.L., Li, X.H., 2016. Integrated in situ U-Pb age and Hf-O analyses of zircon from Suixian Group in northern Yangtze: New insights into the Neoproterozoic low-delta O-18 magmas in the South China Block. Precambr. Res. 273, 151–164.
Yang, Z.N., Yang, K.G., Xu, Y., Deng, X., Cheng, W.Q., Long, Z.Y., 2015. Zircon U-Pb geochronology, Hf isotopic composition, and geological implications of the Neoproterozoic meta-sedimentary rocks in Suizhou-Zaoyang area, the northern Yangtze Block. Sci. China Earth Sci. 58, 1910–1923.
Ye, H.S., Mao, J.W., Xu, L.G., Gao, J.G., Xie, G.Q., Li, X.Q., He, C.F., 2008b. SHRIMP U-Pb dating and geochemistry of the Taishanmiao aluminous A-type granite in Western Henan Province. Geol. Rev. 54, 699–711 (in Chinese with English abstract).
Ye, H.S., Mao, J.W., Li, Y.F., Guo, B.J., Zhang, C.Q., Liu, J., Yan, Q.R., Liu, G.Y., 2008a. SHRIMP zircon U-Pb and molybdenite Re-Os datings of the superlarge donggou porphyry molybdenum deposit in the East Qinling, China, and its geological implications. Acta Geol. Sin.-Engl. 82, 134–145.
Yin, C.Q., Lin, S.F., Davis, D.W., Zhao, G.C., Xiao, W.J., Li, L.M., He, Y.H., 2013. 2.1-1.85 Ga tectonic events in the Yangtze Block, South China: petrological and geochronological evidence from the Kongling complex and implications for the reconstruction of supercontinent Columbia. Lithos 182, 200–210.
Yu, X.Q., Liu, J.L., Li, C.L., Chen, S.Q., Dai, Y.P., 2013. Zircon U-Pb dating and Hf isotope analysis on the Taihua Complex: constraints on the formation and evolution of the Trans-North China Orogen. Precambr. Res. 230, 31–44.
Zeng, L.J., Bao, Z.W., Zhao, T.P., Yao, J.M., Zhou, D., 2013. Geochronology and geochemistry of the Mesoproterozoic Panhe syenites in the southern margin of North China Craton and its tectonic implications. Acta Petrol. Sin. 29, 2425–2436 (in Chinese with English abstract).
Zhang, H., Li, C.Y., Yang, X.Y., Sun, Y.L., Deng, J.H., Liang, H.Y., Wang, R.L., Wang, B.H., Wang, Y.X., Sun, W.D., 2014a. Shapinggou: the largest Climax-type porphyry Mo deposit in China. Int. Geol. Rev. 56, 313–331.
Zhang, H.F., Sun, M., 2002. Geochemistry of mesozoic basalts and mafic dikes, southeastern North China craton, and tectonic implications. Int. Geol. Rev. 44, 370–382.
Zhang, R.Y., Sun, Y., Zhang, X., Ao, W.H., Santosh, M., 2016. Neoproterozoic magmatic events in the South Qinling Belt, China: implications for amalgamation and breakup of the Rodinia supercontinent. Gondwana Res. 30, 6–23.
Zhang, J., Ye, H.S., Zhou, K., Meng, F., 2014b. Processes of ore genesis at the world-class Yuchiling molybdenum deposit, Henan province, China. J. Asian Earth Sci. 79, 666–681.
Zhao, S.J., Li, S.Z., Liu, X., Santosh, M., Somerville, I.D., Cao, H.H., Yu, S., Zhang, Z., Guo, L.L., 2015. The northern boundary of the Proto-Tethys Ocean: Constraints from structural analysis and U-Pb zircon geochronology of the North Qinling Terrane. J. Asian Earth Sci. 113, 560–574.
Zhao, T.P., Zhai, M.G., Xia, B., Li, H.M., Zhang, Y.X., Wan, Y.S., 2004. Zircon U-Pb SHRIMP dating for the volcanic rocks of the Xiong'er Group: constraints on the initial formation age of the cover of the North China Craton. Chinese Sci. Bull. 49, 2495–2502.
Zhao, J.H., Zhou, M.F., Yan, D.P., Zheng, J.P., Li, J.W., 2011. Reappraisal of the ages of Neoproterozoic strata in South China: no connection with the Grenvillian orogeny. Geology 39, 299–302.
Zhu, X.Y., Chen, F.K., Yang, L., Wang, W., Hieu, P.T., Miao, L.C., Zhang, F.Q., 2009. Zircon Hf isotopic composition and source characteristics of the Wudang Group in the Qinling orogenic belt, western Henan province. Acta Petrol. Sin. 25, 3017–3028 (in Chinese with English abstract).
Zhu, X.Y., Chen, F.K., Li, S.Q., Yang, Y.Z., Nie, H., Siebel, W., Zhai, M.G., 2011. Crustal evolution of the North Qinling terrain of the Qinling Orogen, China: evidence from detrital zircon U-Pb ages and Hf isotopic composition. Gondwana Res. 20, 194–204.

Zhu, X.Y., Chen, F.K., Liu, B.X., Siebel, W., 2013. Zircon U-Pb and K-feldspar megacryst Rb-Sr isotopic ages and Sr-Hf isotopic composition of the Mesozoic Heyu pluton, eastern Qingling orogen, China. Lithos 156, 31–40.

Zhu, X.Y., Chen, F.K., Nie, H., Siebel, W., Yang, Y.Z., Xue, Y.Y., Zhai, M.G., 2014. Neoproterozoic tectonic evolution of South Qinling, China: Evidence from zircon ages and geochemistry of the Yaolinghe volcanic rocks. Precambr. Res. 245, 115–130.

Zhu, Y.S., Yang, J.H., Sun, J.F., Wang, H., 2017. Zircon Hf-O isotope evidence for recycled oceanic and continental crust in the sources of alkaline rocks. Geology 45, 407–410.

Zhu, L.M., Zhang, G.W., Guo, B., Lee, B., Gong, H.J., Wang, F., 2010. Geochemistry of the Jinduicheng Mo-bearing porphyry and deposit, and its implications for the geodynamic setting in East Qinling, PR China. Chem. Erde-Geochem. 70, 159–174.